Effect of Elevated PEM Fuel Cell Operating Temperature (120°C and 140°C) and Membrane Thickness on Proton Conductivity for Combat Vehicle Use

Theodore. E. Burye[a]

[a] U.S. Army, Ground Vehicle Systems Center, Warren, Michigan, 48397, USA

Electrical power required to operate vehicles in the U.S. Army is increasing due to expanding mission requirements, such as silent watch, exportable power, and powerful onboard electronics. Proton Exchange Membrane Fuel Cells (PEMFCs) provide a solution, but stack thermal-cycling, electrocatalyst and membrane degradation losses need to be reduced before integration of PEMFCs can be realized. Membrane thermal degradation is exacerbated by poor heat rejection (as ballistic grills impede airflow) which can raise stack temperatures ≥140°C. Commercial PEMFCs operate ~65°C so elevated temperatures could degrade the membrane. Nafion 115 (127 μm), 117 (183 μm) and 1110 (254 μm) membranes submerged in 16 MΩ water were heated between 65-140°C to investigate elevated temperature and membrane thickness on proton conductivity. EIS results showed sample thickness did not statistically impact conductivity overall. Conductivity, however, was impacted for temperatures >100°C with each material. Overall, these materials are not suitable when operating PEMFCs above 100°C.

Introduction

The electrical power required to operate ground combat vehicles in the United States (U.S.) Army is projected to increase due to an expanding set of capabilities and mission duties placed upon current combat vehicles used in an ever changing combat environment. Some of these additional capabilities/duties which are electrical power intensive include silent watch (long term mounted surveillance), advanced radios/jamming devices/sensors, directed energy weapons, exportable power supporting stationary applications, and vehicle-to-grid connectivity applications. Increasing the available electrical power for vehicle operation can be challenging as each vehicle has a limited amount of space, which is already being used for other critical applications. To provide increased electrical power, a compact, power dense and energy efficient source would be needed, so it could fit into the same space claim while still increasing power output for the vehicle. Proton Exchange Membrane Fuel Cells (PEMFCs) are capable of meeting those requirements and thus would be ideal as the primary and/or auxiliary power generator in vehicles for short or long-term missions. While PEMFCs are able to provide power from a compact/power dense source for combat vehicles, there still exists a number of critical issues which need to be resolved before the U.S. Army can integrate PEMFCs effectively. These issues include: 1. Stack thermal-cycling and sealing degradation (1, 2, 3), 2. Electrocatalyst

degradation (4, 5, 6) and 3. Cell membrane thermal degradation (7, 8, 9). In addition, the U.S. Army needs to overcome poor heat rejection from the PEMFC, due to significantly reduced air flow through the ballistic grills. The reduced heat rejection is only magnified as many vehicles operate in locations with elevated ambient temperatures reaching 46°C to 54°C (such as countries in the Middle East). Commercial PEMFCs are typically engineered to operate at temperatures not to exceed 65°C. Operating PEMFCs in vehicles with decreased heat rejection in environments reaching temperatures close to the maximum operating temperature could result in thermal degradation of the polymer membrane. Analysis of these operating conditions predicts the internal stack temperature could reach at least 140°C.

The polymer membrane used in the construction of each cell is a vital component for stack operation since it allows the transport of protons through the membrane while electrons traverse an external circuit and deliver power. Consistent, reliable power output from the stack requires the membrane material to maintain its material properties, such as proton conductivity, over a period of time. To combat material properties changing within the polymer different chemical formulations have been developed (10, 11, 12, 13, 14) with increased chemical and thermal degradation resistances. Nafion®, which is a brand name for a sulfonated tetrafluoroethylene based fluoropolymer-copolymer, is commonly used. Nafion® has a high thermal decomposition temperature of around 300°C (15, 16), which is comparatively high compared to other membrane materials, and the capability of conducting protons (17, 18) which makes it attractive for use in PEMFCs. Since Nafion® has a relatively high thermal decomposition temperature it would appear a suitable choice for PEMFCs operating at temperatures significantly higher than 65°C. However, research has shown that Nafion® may not be as thermally stable as previously thought when stacks are operated at temperatures ≥100°C (19) for extended periods of time. Operating PEMFCs between 120°C and 140°C could result in catastrophic degradation and significant changes in the polymer's proton conductivity, for example. One possible approach to mitigate or reduce membrane thermal degradation would be to engineer cells with thicker membranes, where the added mass would allow the polymer to withstand increased temperature for longer periods of time.

This study had two objectives. The first was to investigate the effect that the temperatures PEMFCs used in combat vehicles would potentially experience, such as 120°C and 140°C, would have on the proton transport capabilities of Nafion® 115. The second was to investigate whether thicker Nafion® membranes, which had same starting properties, could mitigate thermal degradation compared to Nafion® 115. Typical proton conductivity results at 65°C, using the same Nafion® materials, would be used as a baseline to determine the magnitude of material property changes. The baseline proton conductivity of Nafion® at room temperature (21°C) was not compared in this study since the purpose of this analysis was to compare changes at elevated temperatures (120°C and 140°C) against performance data at 65°C which is realistic in the current commercial PEMFC stack technology.

Experimental Methods

Pristine Nafion® 115, 117 and 1110 polymer membrane samples, with a 1.61 cm^2 surface area (1.27 cm x 1.27 cm), were cut from 30 cm x 30 cm sheets of each material (Fuel Cell Store, College Station, TX, USA). These three materials will be referred to 115, 117 and 1110 for the remainder of this paper for simplicity. Samples had starting thicknesses of 127 μm (115), 183 μm (117) and 254 μm (1110) before any experimentation occurred. Next, samples were submerged in 16 MΩ water until fully saturated, then heated (while being saturated) at 65°C, 120°C and 140°C for different periods of time. Heated, saturated samples were then characterized using Electrochemical Impedance Spectroscopy (EIS), sample thickness measurements, proton conductivity calculations, sample water uptake percentage calculations, Fourier-Transform Infrared (FTIR) spectroscopy and X-Ray Diffraction (XRD).

Heating Experiments

Samples were cut from the original 30 cm x 30 cm polymer sheets and submerged in room temperature 16 MΩ water for 1 hour prior to heating to ensure each sample was completely saturated. Submerged samples were heated at 65°C, 120°C and 140°C for 2, 8 and 24 hours. Samples tested at 65°C were heated inside a beaker exposed to air filled with 10 mL of 16MΩ water. Additional water was added periodically to the beaker to ensure each sample stayed submerged and fully saturated. Samples tested at 120°C or 140°C were heated while submerged inside a sealed cylindrical reaction vessel filled with 50 mL of 16 MΩ water. Sealing the reaction vessel allowed the water temperature to exceed 100°C. The reaction vessel was heated using an electric heating ring with a thermocouple placed between the vessel outer wall and the heating ring elements to provide temperature control.

Electrochemical Impedance Spectroscopy (EIS) Experiments

Samples were characterized after each heating experiment using a Solartron SI 1287 Electrochemical Interface attached to a Solartron 1255B Frequency Response Analyzer (Solartron Analytical, Farnborough, Hampshire, UK). Scans were performed using current sweep with a 0 DC voltage, current amplitude of 0.001A and a frequency range from 10^5 to 0.1 Hz. Samples were first saturated in room temperature 16MΩ water for at least 1 hour prior to each EIS measurement. Next, samples had their surface dried to remove any excess water which could influence measurement results. Rectangular sections were then cut, using a punch, from each heated sample to perform EIS measurements. Each section measured 0.979 cm in length and 0.869 cm in width. Finally, electrical contacts were attached to each end of the section being measured. Samples were placed into room temperature 16MΩ water between each EIS measurement to maintain a constant level of water saturation. At least three sections were cut from each sample and averaged to account for possible variations that could exist from the instrument or processing conditions.

Nyquist plots were generated from the collected EIS raw data where the imaginary AC impedance component was plotted on the y-axis and real AC impedance component was plotted on the x-axis.

Sample Thickness Measurements

Sample thicknesses were measured using a caliper after each heating experiment to account for changes in water uptake which may influence proton conductivity calculations. Samples were first placed in room temperature 16MΩ water for at least 1 hour and then each saturated sample thickness was measured across the sample surface.

Proton Conductivity Calculations

Sample proton conductivity was calculated using Equation 1 and Equation 2 shown below:

$$\sigma = \frac{L}{R*A} \quad [1]$$

$$A = W * T \quad [2]$$

where σ is the proton conductivity of each sample in S/cm, L is the length of each sample in cm, R is the ohmic resistance determined from raw EIS measurements (the distance on the x-axis between the initial x-intercept and the origin) in Ω, A is the cross sectional area of proton conduction for each sample in cm^2, W is the width of each sample in cm and T is the thickness of each sample in cm.

Water Uptake Percentage Calculations

Sample water uptake percentage values were calculated using the following experimental procedure after each heating experiment. First, samples were placed inside an automatic desiccator (Bel-Art – SP Scienceware, South Wayne, NJ, USA) for at least 3 hours to dry each sample to a relative humidity <10%. Samples were then removed from the desiccator and their dry mass was measured using a Mettler Toledo analytical balance (Mettler Toledo, Columbus, OH, USA) with a 0.1 mg mass resolution. Next, samples were submerged and saturated in room temperature 16MΩ water for at least 1 hour, had their surface dried, and then had their mass re-measured using the analytical balance. Finally, water uptake percentages were calculated on a mass basis by comparing the dry and saturated masses after heating experiments.

Fourier-Transform Infrared (FTIR) Spectroscopy Experiments

Samples were characterized after each heating experiment using a Thermo Scientific Nicolet 6700 system (Thermo Scientific Instruments Corporation; Madison, WI, USA). Scans were performed between 4000 and 675 cm^{-1} wavenumbers, using a Germanium crystal and 64 scans were performed per sample.

X-Ray Diffraction (XRD) Experiments

Samples were characterized after each heating experiment using a SmartLab X-ray Diffraction (XRD) system (Rigaku Americas Corporation; The Woodlands, TX, USA). Broad material scans were conducted using a 20kV voltage, $5° \leq 2\theta° \leq 90°$ scan range, 0.040 step width, 1.00°/min scan speed, copper filament and nickel filter.

Results

Figure 1 shows the raw EIS data from the 115, 117 and 1110 samples after being heated at 65°C, 120°C and 140°C for 2, 8 and 24 hours plotted on Nyquist plots. The raw EIS data represents the average results observed for each experiment but does not represent variations in standard deviation, which are shown in the next figure. Overall, all samples decreased their ohmic resistance (distance between the x-intercept and the origin) as temperatures were increased to 120°C and 140°C, when compared to 65°C. This change in ohmic resistance was diminished more as the sample thickness increased, on average. The ohmic resistance remained relatively constant with time when samples were heated at 65°C or 120°C, but the ohmic resistance, for thicker samples (117 and 1110) at 140°C, appeared to increases slightly after 24 hours, compared to the 120°C results.

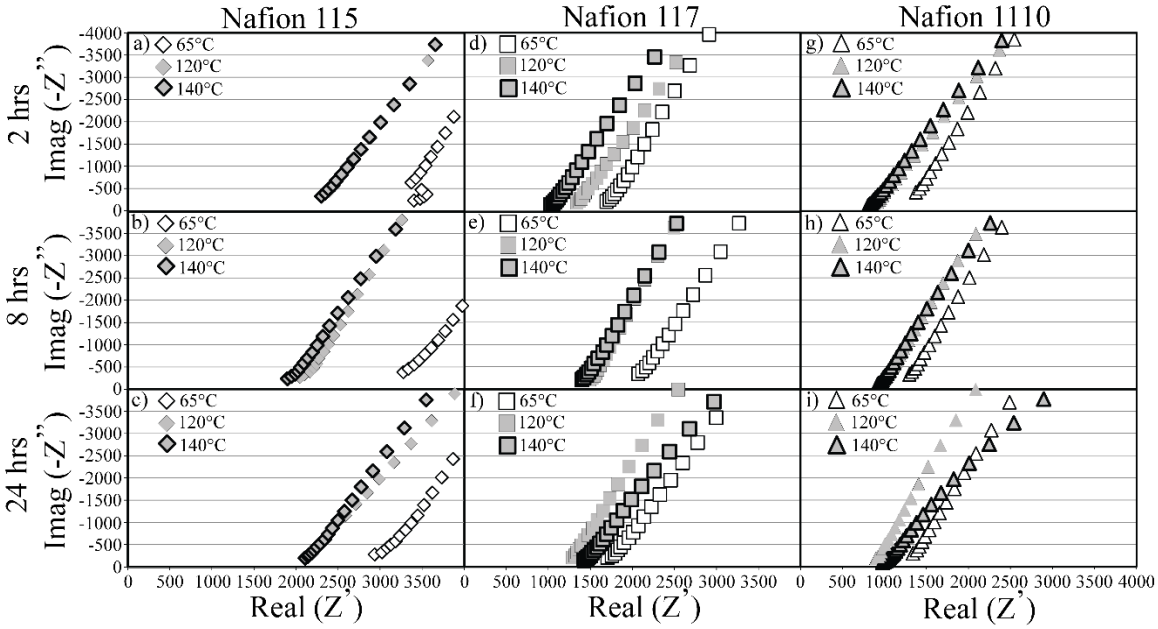

Figure 1: Raw EIS data of (a-c) 115, (d-f) 117 and (g-i) 1110 heated at 65°C, 120°C and 140°C. Samples were heated at each temperature for 2 hours (a, d, g), 8 hours (b, e, h) and 24 hours (c, f, i).

Figure 2 shows the calculated ohmic resistance values from Figure 1, including standard deviations, for the heated samples. Overall, the data trends observed in Figure 1 are seen here as well. The ohmic resistance decreased as the temperature was increased for each material thickness. The only exception was that the data showed statistically the same trends for each material thickness as a function of time at 140°C, which was different.

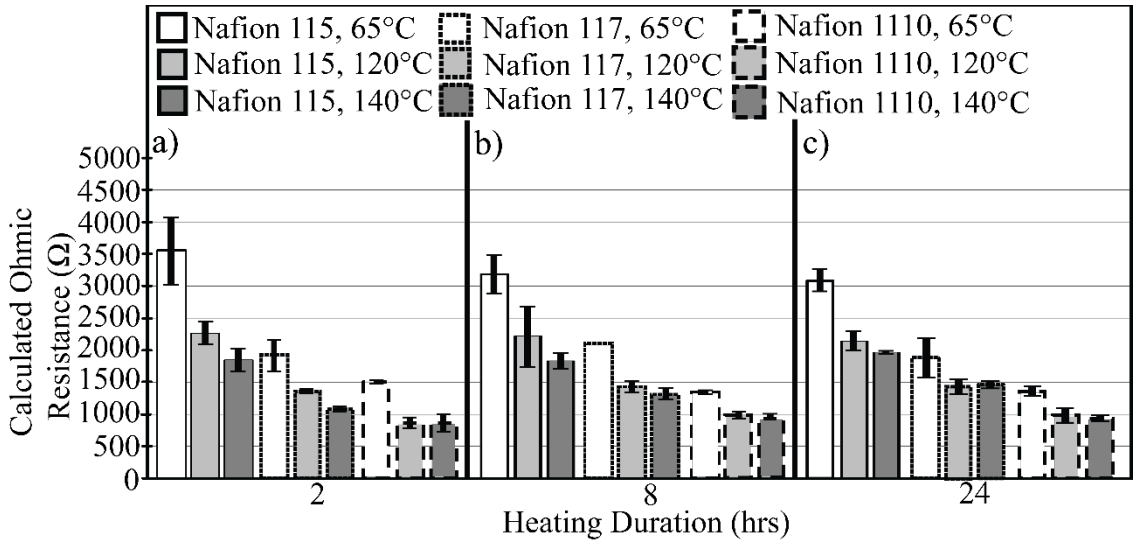

Figure 2: Calculated ohmic resistance values from raw EIS data collected from (a-c) 115, (a-c) 117 and (a-c) 1110 samples. All samples were heated at 65°C, 120°C and 140°C for (a) 2 hours, (b) 8 hours and (c) 24 hours.

Figure 3 shows the measured sample thickness (due to changes in water uptake) from the 115, 117 and 1110 samples after being heated at 65°C, 120°C and 140°C for 2, 8 and 24 hours. Overall, the sample thickness increased with temperature for each material, but remained relatively constant with time at each temperature, for each material. Slight changes in sample thickness were observed over time for each material, but those changes were small and no trends could be observed. In addition, larger percentage changes in sample thickness were observed as the initial sample material thickness increased (i.e. 115 showed a smaller percentage increase in thickness than 1110 did). The 115 showed an average increase of 14.77% when heated to 140°C (compared to 65°C), while the 1110 showed an average increase of 27.93%, which is nearly double.

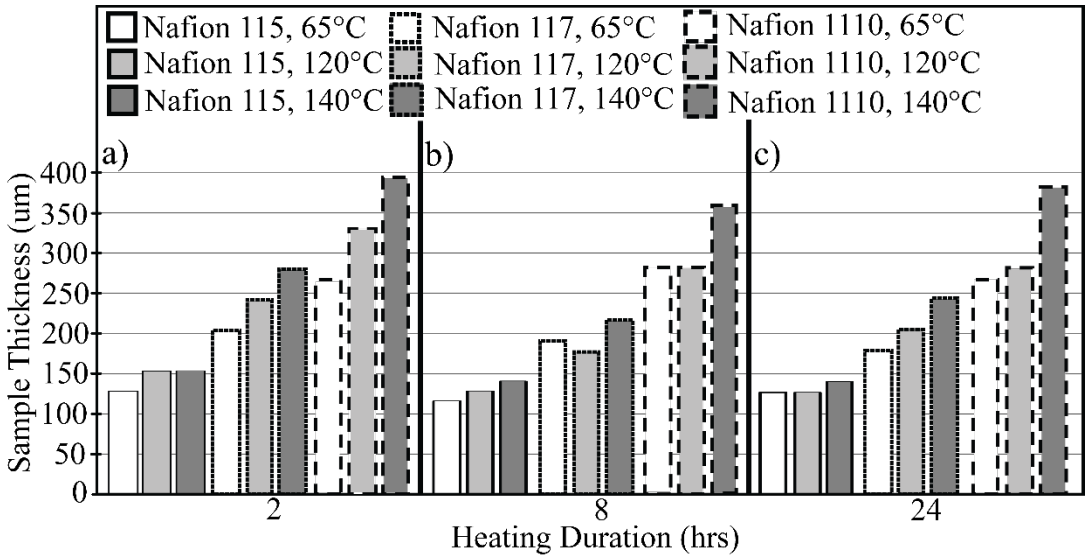

Figure 3: Measured sample saturated thickness values from (a-c) 115, (a-c) 117 and (a-c) 1110 samples. All samples were heated at 65°C, 120°C and 140°C for (a) 2 hours, (b) 8 hours and (c) 24 hours.

Figure 4 shows the calculated proton conductivity from the 115, 117 and 1110 samples after being heated at 65°C, 120°C and 140°C for 2, 8 and 24 hours, which was determined using Equation 1. The sample length and width was 0.979 cm and 0.869, respectively. In addition, the ohmic resistance values were calculated from the raw EIS data (Figure 1 and Figure 2) and the sample thickness values were used from Figure 3. Overall, the calculated proton conductivity increased as the temperature was increased for all initial material thicknesses. This increase in proton conductivity with increased temperature statistically stays constant with heating duration as well, except for the 117 and 1110 which appear to lower their proton conductivity after 24 hours of 140°C heating, compared to the 8 hour results.

Internal structural changes to the polymer samples, such as increased structural disorder or changes to the active vibration modes, are hypothesized to cause the increase in proton conductivity and will be analyzed next. A severely disordered polymer network could explain the decreased proton conductivity while heating at 140°C for 24 hours, if the polymer was damaged to the point where proton conduction was hindered. Alternatively, changes to active vibrational modes could increase or decrease how effectively the polymer interacts and retains water.

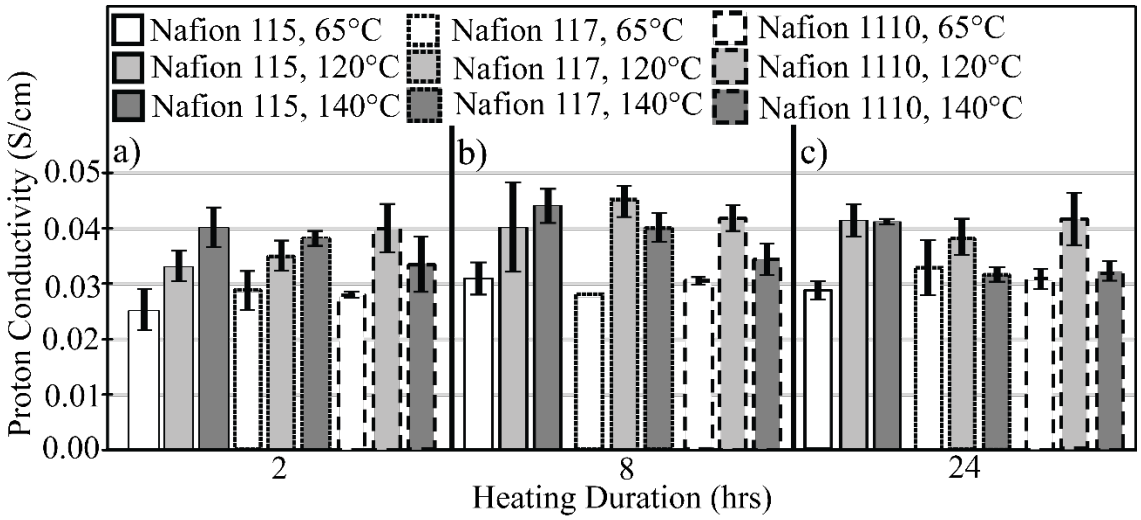

Figure 4: Calculated proton conductivity values from (a-c) 115, (a-c) 117 and (a-c) 1110 samples. All samples were heated at 65°C, 120°C and 140°C for (a) 2 hours, (b) 8 hours and (c) 24 hours.

Figure 5 shows the measured water uptake percentage from the 115, 117 and 1110 samples after being heated at 65°C, 120°C and 140°C for 2, 8 and 24 hours. Overall, the water uptake percentage for each separate material sample was similar when heated at 65°C as a function of time, but changed at elevated temperatures. The largest factor influencing the water uptake for all the sample thickness values was temperature and increasing the operating temperature increased the amount of water inside the polymer sample. Another trend, which is not as noticeable, is the water uptake was slightly higher (at constant heating duration and temperature) for samples that started with an increased thickness (i.e. 1110 increased its water uptake more than 115). Increased water content within the samples could potentially be caused by two different things for increased proton transport. These

two possibilities include an increased disorder within the polymer network or different vibrational modes being present which have more affinity for retaining water within the polymer network. Both of these possibilities will be investigated to determine if one or both are present in each sample.

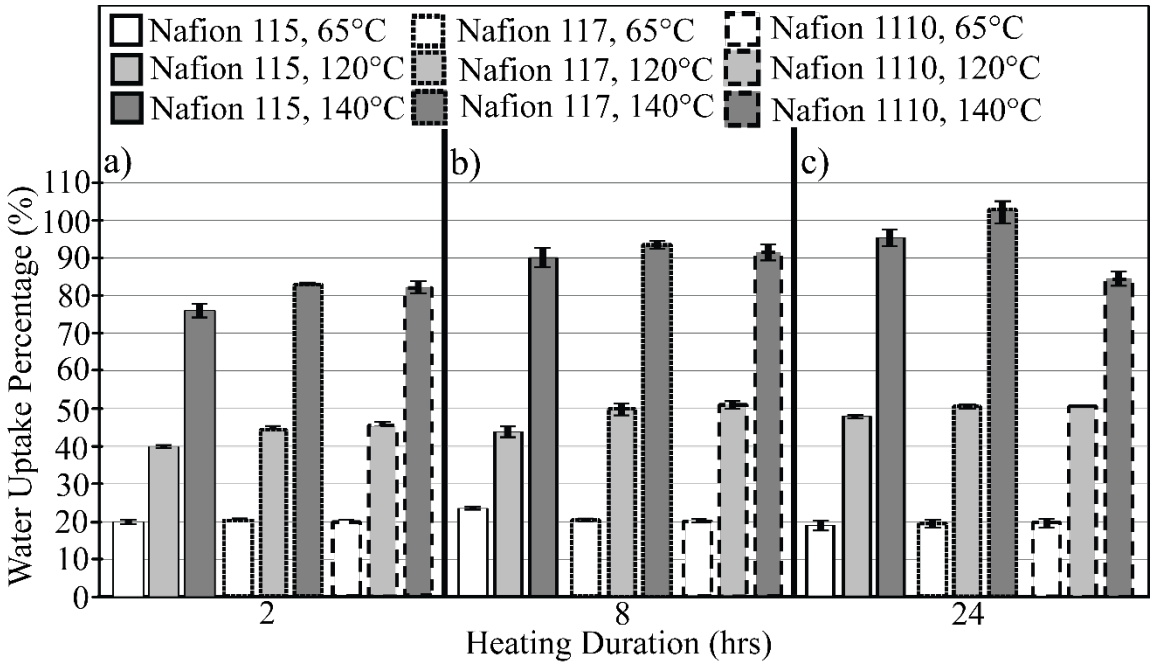

Figure 5: Measured water uptake percentages from (a-c) 115, (a-c) 117 and (a-c) 1110 samples. All samples were heated at 65°C, 120°C and 140°C for (a) 2 hours, (b) 8 hours and (c) 24 hours.

Figure 6 shows the XRD scans from the 115, 117 and 1110 samples after being heated at 65°C, 120°C and 140°C for 2, 8 and 24 hours. Two peaks were detected, located at 16.7° and 39.3° 2-Theta, within all three samples. These peaks will be referred to as Peak I and Peak II, respectively. Overall, two trends were observed which indicate heating the samples resulted in increased internal disorder within the material. First, both peak I and II showed increased broadening after being heated. Peak broadening, at least with crystalline nanoparticles, indicates decreased grain/particle size (20, 21). Increased peak broadening in crystalline/semi-crystalline polymers has been shown the polymer is becoming more disordered (22, 23), while there are multiple types "disorder" which result in polymer peak broadening. It is hypothesized the increased sample disorder is caused, at least partially by depolymerization (24, 25), however determination of the exact mechanism is outside the scope of the study. Increased disorder within the polymer structure could lead to initially increased proton conduction, but then would limit conduction as the polymer network is disrupted further. Second, the increased peak broadening generally was observed to be more prevalent at increased heating temperatures or increased periods of time. This would also make sense as increased temperature and/or time would increase the amount of disorder within each polymer sample and could explain the increased proton conductivity.

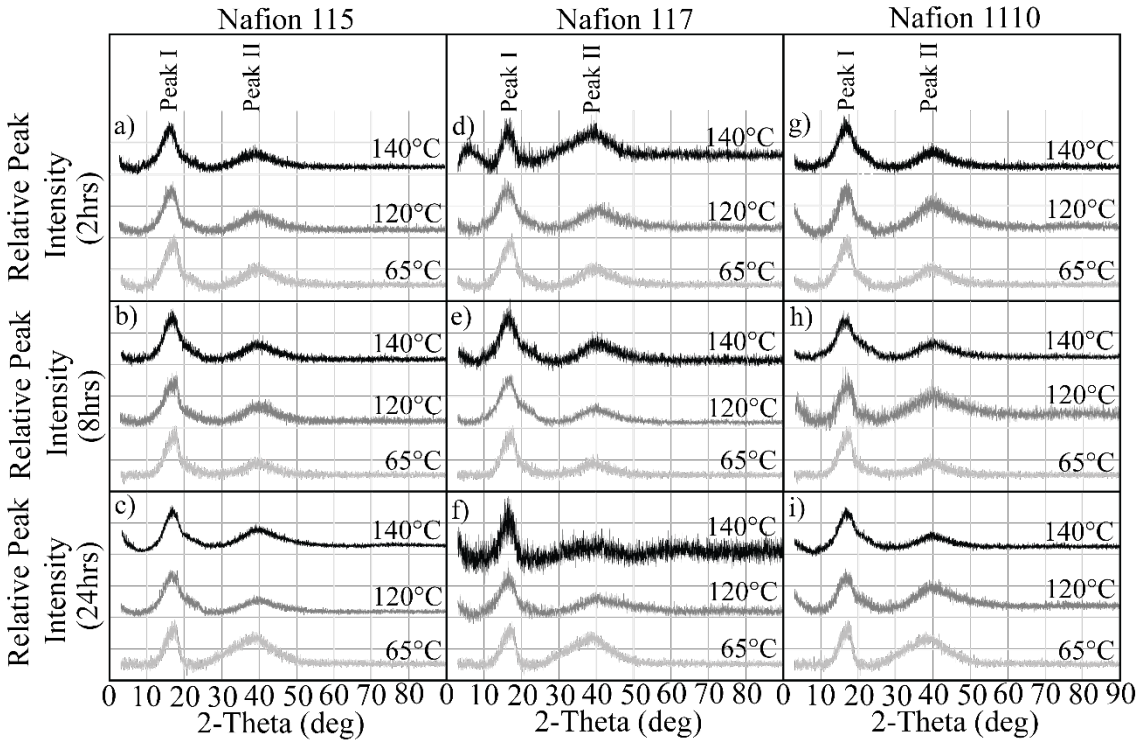

Figure 6: XRD spectra from (a-c) 115, (d-f) 117 and (g-i) 1110 samples. All samples were heated at 65°C, 120°C and 140°C for (a, d, g) 2 hours, (b, e, h) 8 hours and (c, f, i) 24 hours.

Figure 7 shows the FTIR scans from the 115, 117 and 1110 samples after being heated at 65°C, 120°C and 140°C for 2, 8 and 24 hours. Overall, all three FTIR scans were the same after being heated at 65°C for any length of time. Changes to the internal vibrational modes started to become apparent after being heated at 120°C. After only 2 hours of heating at 120°C these changes were most apparent with the 117 and 1110 samples. At 2 hours of heating there were no new vibration modes observed, but the 1307, 1203, 1149, 1060, 979 and 968 cm^{-1} peaks all showed changes to their peak intensity ratios. As more time passed, while heating at 120°C, all three materials showed changes to their vibrational modes. Generally, differences include changes to peak intensity ratio values, but new vibrational modes do eventually appear after heating for 24 hours at 120°C, located at 1014 cm^{-1} for the 117 and 1110 samples. Samples that were heated at 140°C showed multiple and severe changes to the internal vibrational modes present for all the materials. These changes, as with the 120°C results, were more pronounced with the 117 and 1110 after only 2 hours of heating. Results after heating at 140°C are more dramatic. The additional vibration mode, located at 1014 cm^{-1} appears after heating for only 2 hours, where it 24 hours at 120°C. Changes to peak intensities are present as well but do not appear to be as dominant. All of these observations indicate the dominant vibrational modes, produced by the different functional groups within the polymer, are being switched around. These switches also impact the functional groups that are dominant, which interact with water differently and could explain the increased proton conductivity.

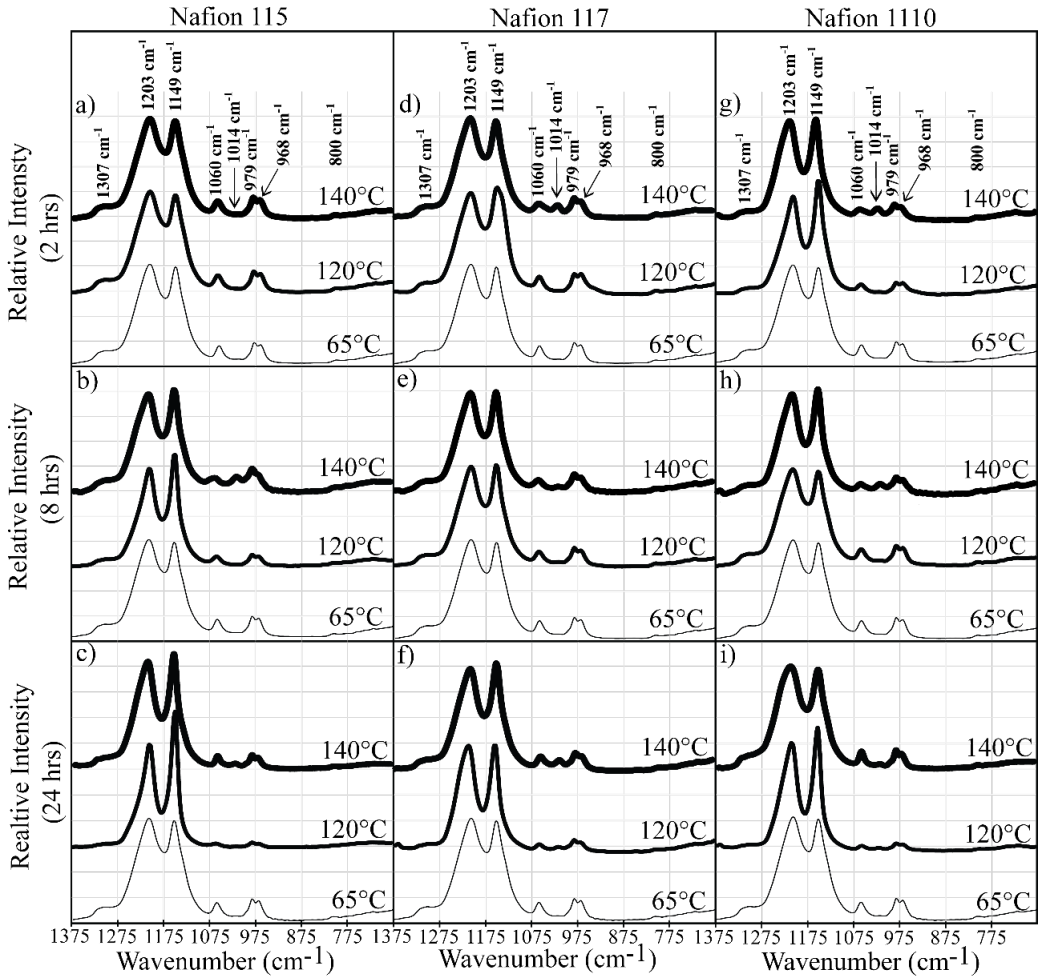

Figure 7: FTIR spectra from (a-c) Nafion 115, (d-f) Nafion 117 and (g-i) Nafion 1110 samples. All samples were heated at 65°C, 120°C and 140°C for (a, d, g) 2 hours, (b, e, h) 8 hours and (c, f, i) 24 hours.

Conclusions

Heating Nafion® 115, 117 and 1110 samples at 120°C and 140°C has been shown to drastically change the proton conductivity beyond what is observed when operating at 65°C. Heated >100°C for 2 hours showed increased conductivity for all three samples when compared to being heated at 65°C, but proton conductivity stabilized or decreased after 24 hours of heating (primarily for the 117 and 1110). Increases in conductivity were generally greater with increased temperature and when testing thinner materials, such as 115. Changes to the calculated proton conductivity are primarily determined by the material ohmic resistance and sample thickness. Decreasing the ohmic resistance and/or sample thickness can both result in increased proton conductivity. However, conductivity can also be decreased, or become stagnant, if the rate of change of these parameters changes.

Proton conductivity for the thinner samples, such as 115, was primarily influenced by its ohmic resistance as that decreased over time while its sample thickness remained relatively constant as a function of time. Conductivity for the 117 and 1110 samples

appeared to be influenced by both their ohmic resistance and sample thicknesses as a function of time.

Changes to sample ohmic resistance and thickness appear to be related to increased structural disorder and changes to active vibrational modes within each sample. It is hypothesized that the increased structural disorder promotes increased conductivity pathways initially, but as time passes enough degradation occurs where the diffusion distance between polymer chains becomes too large for protons to be conducted. The changes to the active vibrational modes influence how effectively samples can interact and retain water and proton, which increase or decrease proton conductivity as time passes.

These results illustrate that, while Nafion® has one of the highest decomposition temperatures for polymers being used in PEMFCs currently, it is not completely immune to the effects of degradation at temperatures >100°C for commercially available membrane thicknesses. Even current recommended operating temperatures at 65°C can result in significant material property changes, while temperatures >100°C resulted in severe material changes. Overall, consistent material properties are required for useful power to be provided in combat applications. Due to these results, PEMFCs used in combat vehicles for the U.S. Army should investigate alternative polymer materials used in place of Nafion®, which do not change their material properties when operated within the 100°C-150°C temperature range.

Nomenclature

A	Sample cross sectional area (cm^2)
EIS	Electrochemical Impedance Spectroscopy
FTIR	Fourier Transform Infrared
L	Sample length (cm)
σ	Proton conductivity (S/cm)
PEMFC	Proton Exchange Membrane Fuel Cells
R	Ohmic resistance (Ω)
T	Sample thickness (cm)
W	Sample width (cm)
XRD	X-Ray Diffraction

Acknowledgments

The author would like to thank the following individuals for their assistance and use of equipment. Demetrios Tzelepis from the Material Characterization/Failure Analysis group within the Ground Vehicle Systems Center (GVSC) provided technical assistance and use of the XRD equipment. William Roland and Chris Tolliver from the Material Characterization/Failure Analysis group within GVSC allowed use of the FTIR equipment. David Skalny and Tony Thampan from the Energy Storage group within GVSC provided the EIS equipment and technical assistance setting up the EIS.

References

1. T. Søndergaard, L.N. Cleemann, L. Zhong, H. Becker, T. Steenberg, H.A. Hjuler, L. Seerup, Q. Li, J.O. Jensen, *Electrocatalysis*, **9**, (3), 302-313, (2018)
2. T. Mittermeier, A. Weiß, F. Hasché, G. Hübner, H.A. Gasteiger, *J. Electrochem. Soc.*, **164**, (2), F127-F137, (2017)
3. A. Kannan, A. Kabza, J. Scholta, *J. Power Sources*, **277**, 312-316, (2015)
4. M. Cai, M.S. Ruthkosky, B. Merzougui, S. Swathirajan, M.P. Balogh, S.H. Oh, *J. Power Sources*, **160**, (2), 977-986, (2006)
5. Y. Shao, G. Yin, Y. Gao, *J. Power Sources*, **171**, (2), 558-566, (2007)
6. T.E. Burye, *Int. J. Hydrog. Energy*, (2019), DOI: 10.1016/j.injhydene.2019.11.232
7. A. Collier, H. Wang, X.Z. Yuan, J. Zhang, D.P. Wilkinson, *Int. J. Hydrog. Energy*, **31**, (13), 1838-1854, (2006)
8. J. Zhang, Z. Xie, J. Zhang, Y. Tang, C. Song, T. Navessin, Z. Shi, D. Song, H. Wang, D.P. Wilkinson, Z.-S. Liu, S. Holdcroft, *J. Power Sources*, **160**, (2), 872-891, (2006)
9. J. Tan, Y.J. Chao, M. Yang, C.T. Williams, J.W. Van Zee, *J. Mater. Eng. Perform.*, **17**, (6), 785-792, (2008)
10. F. Pereira, K. Vallé, P. Belleville, A. Morin, S. Lambert, C. Sanchez, *Chem. Mater.*, **20**, (5), 1710-1718, (2008)
11. G. Sasikumar, J.W. Ihm, H. Ryu, *Electrochim. Acta*, **50**, (2-3), 601-605, (2004)
12. J. Lobato, P. Cañizares, M.A. Rodrigo, C. Ruiz-López, J.J. Linares, *J. Appl. Electrochem.*, **38**, (6), 793-802, (2008)
13. J. Lobato, P. Cañizares, M.A. Rodrigo, C.-G. Piuleac, S. Curteanu, J.J. Linares, *Int. J. Hydrog. Energy*, **35**, (15), 7889-7897, (2010)
14. D. Ergun, Y. Devrim, N. Bac, I. Eroglu, *J. Appl. Polym. Sci.*, **124**, (S1), E267-E277, (2012)
15. F. Lu, X. Gao, X. Yan, H. Gao, L. Shi, H. Jia, L. Zheng, *ACS. Appl. Mater. Interfaces*, **5**, (15), 7626-7632, (2013)
16. A. Ozden, M. Ercelik, Y. Ozdemir, Y. Devrim, C.O. Colpan, *Int. J. Hydrog. Energy*, **42**, (33), 21501-21517, (2017)
17. Y. Sone, P. Ekdunge, D. Simonsson, *J. Electrochem. Soc.*, **143**, (4), 1254-1259, (1996)
18. A.G. Ivanova, P.A. II'in, A.A. Dmitrieva, O.A. Zagrebelnyy, A.Yu. Gruzinov, G.P. Kopitsa, I. Yu. Kruchinina, O.A. Shilova, *Glass Phys. Chem.*, **42**, 637-639, (2016)
19. S.R. Samms, S. Wasmus, R.F. Savinell, *J. Electrochem. Soc.*, **143**, (5), 1498-1504, (1996)
20. T. Ungár, *Scr. Mater.*, **51**, (8), 777-781, (2004)
21. R. Yogamalar, R. Srinivasan, A. Vinu, K. Ariga, A.C. Bose, *Solid State Commun.*, **149**, 1919-1923, (2009)
22. B. Crist, J.B. Cohen, *J. Polym. Sci.*, **17**, 1001-1010, (1979)
23. N.S. Murthy, H. Minor, *Polymer*, **36**, (13), 2499-2504, (1995)
24. H.K. No, J.W. Nah, S.P. Meyers, *J. Appl. Polym. Sci.*, **87**, (12), 1890-1894, (2003)
25. S. Enthaler, R. Kretschmer, *ChemSusChem.*, **7**, (7), 2030-2036, (2014)